Simultaneous Multi-Element Electrothermal Atomic Absorption Determination Using a Low Resolution CCD Spectrometer and Continuum Light Source: The Concept and Methodology

Dimitri A. Katskov* and G. Eunice Khanye

Department of Chemistry and Physics, Tshwane University of Technology, Pretoria, 0001 South Africa.

Received 11 February 2010, accepted 3 May 2010.

ABSTRACT

A low resolution CCD spectrometer with continuum light source and fast-heated graphite tube atomizer was employed for simultaneous multi-element determination by electrothermal atomic absorption spectrometry (SMET AAS). The sample vaporization pulse was monitored by fast scanning of vapour spectra within the 190–410 nm wavelength range; absorption was measured at the CCD pixels corresponding to atomic resonance lines; function absorbance *vs.* concentration of atomic vapour was automatically linearized, and the modified signals integrated. The setup consisted of a D_2 or Xe arc lamp, a spectral instrument with a half-width of transmittance profile 120 pm, a linear CCD array attached to a PC and a tube atomizer furnished with a carbon fibre collector. In the experiments simultaneous determination of 18 elements was performed in the mixed solutions at the mg L^{-1} to μg L^{-1} level, within 4–4.5 orders of magnitude linear concentration range. About 1–2 min was needed for the measurement and calculation. Limits of detection (LOD) for individual elements were 1.5–2 orders of magnitude higher than those in the single element ET AAS, but similar or below those in flame AAS. Further reduction of LODs and correction of possible spectral and chemical interferences are associated with optimization of the light source and atomization programme and modification of the calculation algorithm.

KEYWORDS

Electrothermal atomic absorption spectrometry, simultaneous multi-element determination, CCD spectrometer, fast-heated graphite tube atomizer.

1. Introduction

Fast development and broad distribution of ICP-OES and ICP-MS instrumentation for multi-element analysis causes reservations regarding the future of electrothermal atomic absorption spectrometry (ET AAS) in its currently most popular modification. The main reason for this situation is the outdated 'single element' concept of traditional AAS methodology, which requires sequential exchange of spectral lamps according to the number of elements to be determined, and the use of analyte masses consistent with the sensitivity of the atomic line and the linearity range of the respective characteristic curve. Nevertheless, ET AAS still remains cost-effective and in its core less prone to interferences when compared with other methods of analytical atomic spectrometry.

Substantial progress in AAS methodology occurred recently when the concept of high resolution continuum light source (HR-CS) AAS was introduced and associated instrumentation developed.[1–3] In the HR-CS AAS instruments (the prototype built in ISAS, Berlin, Germany[2] and its commercial analogue, ContrAA 700 spectrometer, Analytik, Jena, Germany[3]) the element determination is performed using a high intensity continuum light source, high resolution double echelle monochromator (spectral resolution, or full width at half maximum (FWHM) of the transmittance profile is 2.7 pm[2]) with charge coupled device (CCD) detection. The spectral area about 1 nm adjacent to the analytical line of the element to be determined is selected for the measurements, and the radiation monitored within this area using a linear 500 pixel CCD array and data acquisition frequency sufficient for processing a 1–3 s vaporization pulse typical for graphite tube ET AAS. The use of a single light source and automatic readjustment of analytical lines makes possible fast sequential determination of several elements.

The lines of multiple elements can be detected with the HR-CS instruments and used for true simultaneous determination only if they belong to the selected narrow spectral area; however, the number of lines which meet this requirement is limited; the determination sensitivity with those lines is normally much lower than that for the sensitive lines situated beyond the scanned interval.[4] To provide really simultaneous multi-element electrothermal (SMET) AAS, determination of several elements from a single sample spectral range between 190 and 400 nm is needed. The monitoring of the entire wavelength region of analytical interest with high spectral resolution is, indeed, possible by means of an echelle-based spectrograph, [2] but its combination with an ET atomizer would require extremely fast CCD detection and reading that would heavily contribute to the cost of the instrument. These presumptions compel one to look more attentively to the characteristics of low cost, low resolution CCD instruments and the opportunities of their coupling with a continuum light source and ET atomizer for simultaneous multi-element atomic absorption determination.

2. Theory and Estimations

The following excerpts from the theory should help to estimate the impact of spectral resolution on the characteristics of a low

*To whom correspondence should be addressed. E-mail: katskovda@tut.ac.za

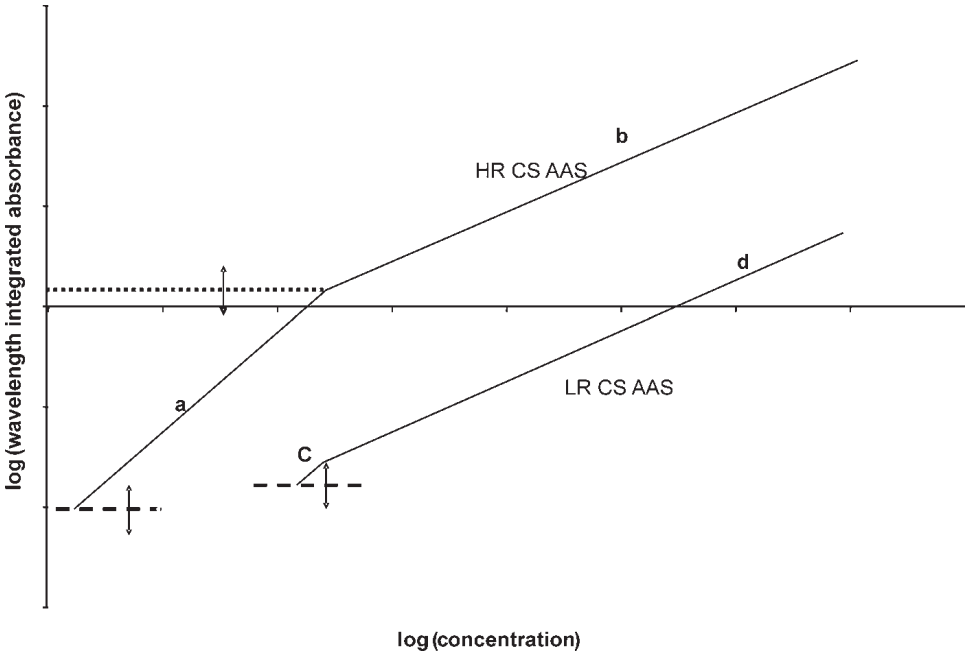

Figure 1 Theoretically predicted behaviour of the calibration curves for (a, b) HR and (c, d) LR CS AA spectrometers. The dotted line indicates the level of conversion of function $S_t \sim N_t$ into $S_t \sim N_t^{0.5}$; the dashed lines show the lowest detectable absorbance.

resolution continuum source (LR-CS) ET AAS instrument.[6]

The presence of N_t atoms in the absorption volume causes absorption within the line profile $A_t(\lambda)$; the profile is broadened due to the transmittance profile $F(\lambda)$ of the spectral instrument. The wavelength distribution of the detected absorbance, $\overline{A}_t(\lambda)$ is determined by convolution of the original line and instrumental transmittance profiles.

$$\overline{A}_t(\lambda) = \int_{-\infty}^{\infty} F(\lambda')A_t(\lambda - \lambda')d\lambda'. \quad (1)$$

If the original half-width of the absorption line is smaller, or at least comparable with, the half-width of the instrumental profile (e.g. for HR spectrometers[2,3]), then

$$\overline{A}_t(\lambda) \cong A_t(\lambda). \quad (2)$$

If the ET vaporizer provides complete atomization of the analyte, then the full amount of the analyte in the sample (N_0) can be found by temporal integration

$$N_0 = \alpha(\lambda)\int_0^{\infty}(A_t(\lambda)/\tau)dt, \quad (3)$$

where $\alpha(\lambda)$ is the sensitivity constant at the respective wavelength and τ is the residence time of atoms in the absorption volume. If τ remains constant during the vaporization and vapour transport, the ratio $\alpha(\lambda)/\tau$ can be determined using reference samples.

For an instrument with a broad instrumental profile (LR spectrometer)

$$\overline{A}_t(\lambda) \cong F(\lambda)\int_{-\infty}^{\infty} A_t(\lambda')d\lambda' = F(\lambda)S_t, \quad (4)$$

where

$$S_t = \int_{-\infty}^{\infty} A_t(\lambda)d\lambda \quad (5)$$

is the wavelength integrated absorbance. Taking Equations (2) and (4) as criteria, in the context of this work a LR spectrometer can be defined as an instrument having a transmittance profile 50 or more times broader than the original absorption lines under ET AAS conditions. For a LR spectrometer at any point of the resulting line profile, the absorbance $\overline{A}_t(\lambda)$ is proportional to S_t; and the absorbance maximum is reduced, compared with that for a HR instrument, to a degree depending on the width of the instrumental profile $F(\lambda)$. The determination sensitivity should become at least 50 times lower compared with a HR spectrometer; therefore, higher amounts of the analyte should be introduced in the atomizer, or the atomizer should provide a higher density of atomic vapour to obtain a measurable signal.

According to the theory and experimental data,[1,2,7] high analyte vapour content in the absorption volume causes full absorption in the centre of the line; further increase of absorption occurs on account of the wings of the line. The vaporization of large amounts of the analyte is accompanied by a change of the function S_t *vs.* N_t, depending on the concentration of atomic vapour in the absorption volume. Above some level it changes from $\overline{A}_t(\lambda) \sim S_t \sim N_t$ to $\overline{A}_t(\lambda) \sim S_t \sim N_t^{0.5}$ (see Fig. 1, curves a and b); the upper border of the linearity range $S_t \sim N_t$ (dotted line) depends on the individual characteristics of the atomic line and on stray light. According to the data for Pb, Cd and Ag lines,[1] the range is limited from above by the condition $\overline{A}_t < 1$ to 1.3. The combined function $S_t = f(N_t)$ below and above this limit cannot be quantitatively predicted. This uncertainty does not permit temporal integration of the absorption pulses for the quantification of the ET AAS measurements if the absorbance exceeds the indicated level. The minimal detectable signal and the lower border of the linear determination range are determined by the level of absorption fluctuations (Fig. 1, dashed lines), which depends on the intensity and wavelength distribution of the radiation output of the continuum spectrum light sources, the stability of the light flux, the efficiency of the atomizer and other factors characteristic for AA spectrometry.[8]

According to the estimation above, for a LR instrument the interception point of the curves $S_t \sim N_t$ and $S_t \sim N_t^{0.5}$ is shifted to the area below $\overline{A}_t = 0.02$ to 0.025 (Fig. 1, curves c and d). If this value is close to the noise level and the density of atomic vapour in the atomizer is sufficient to provide the condition $\overline{A}_t \geq 0.02$ to 0.025, then only part of the combined function, which is $\overline{A}_t \sim S_t \sim N_t^{0.5}$, remains significant. For the area above the interception point

$$N_t \sim [\overline{A}_t(\lambda)]^2. \quad (6)$$

If the interception point is situated close to the detection level,

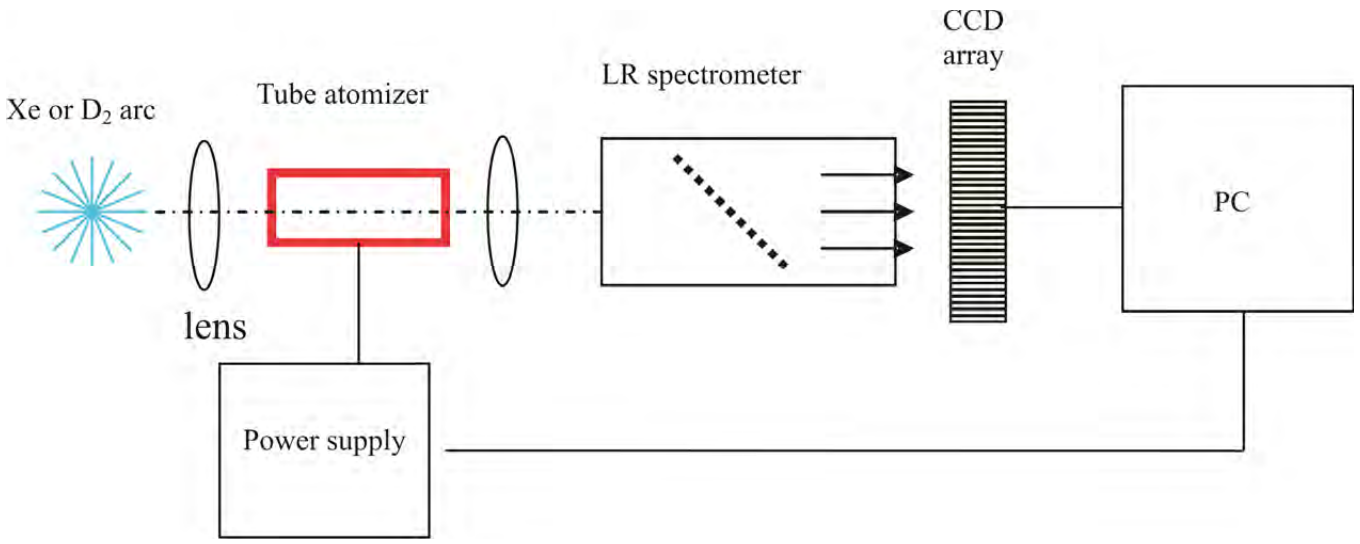

Figure 2 Experimental setup.

a modification of Equation (6) can be suggested,

$$N_t \sim [\overline{A}_t(\lambda)]^2\, \varphi[\overline{A}_t(\lambda)] \qquad (7)$$

where $\varphi = +1$ or -1, if $[\overline{A}_t(\lambda)] > 0$ or < 0, respectively. For the signals exceeding the noise level Equation (7) reduces to Equation (6). Otherwise, according to Equation (7), short noise causes random deviations of absorbance around the zero line. Similarly to Equation (3), under conditions of full atomization and constant residence time of atoms in the absorption volume the total amount of the analyte element e in the sample can be found,

$$N_{0e} = [\alpha_e(\lambda_e)/\tau_e]\int_0^\infty [\overline{A}_t(\lambda_e)]^2\, \varphi[\overline{A}_t(\lambda_e)]dt\,, \qquad (8)$$

where λ_e is the wavelength of the absorption line.

For an instrument with CCD array detection

$$\overline{A}_t(\lambda) \cong \overline{A}(p,n) = \log[I_0(p,n)/I(p,n)]\,, \qquad (9)$$

where $I(p,n)$ and $I_0(p,n)$ are the electric outputs of a CCD pixel p in spectrum n in the presence and absence of sample vapour in the vaporizer. Consequently,

$$N_t \sim [\overline{A}(p,n)]^2 \varphi[\overline{A}(p,n)] = \boldsymbol{A}(p,n) \qquad (10)$$

and Equation (8) can be modified to

$$N_{0e} \cong \alpha_{pe}\theta/\tau_e \sum_n [\overline{A}(p_e,n)]^2\, \varphi[\overline{A}(p_e,n)]$$

$$= \alpha_{pe}(\theta/\tau_e)\sum_n \boldsymbol{A}(p_e,n)\,, \qquad (11)$$

where α_{pe} and $\overline{A}(p_e,n)$ are equal to $\alpha_e(\lambda)$ and $\overline{A}_t(\lambda_e)$, averaged over the spectral interval of one pixel; θ is the data acquisition period; and n is the scan number. Equations (9) to (11) can be automatically applied to any pixel within the $I_0(p,n)$ and $I(p,n)$ data matrices obtained in the experiment. Information regarding the content of a particular element in the sample can be found using linearization, Equation (10), and summation of absorbance data at pixel p_e, corresponding to the resonance line of the element, Equation (11).

Thus, the matrix of $\boldsymbol{A}(p,n)$ data and the set of respective coefficients $a_{pe}(\theta/\tau_e)$ independently determined should permit the simultaneous determination of several elements. The range of applicability of Equation (11) in practice depends on the spectral resolution of the CCD instrument, the ability of the atomizer to create a high concentration of atomic vapour in the absorption volume and the output of the light source at a specific wavelength.

Since Equation (7) can be applied to any pixel within the broadened absorption line profile, the pixels at a distance δ from the maximum can be used for background correction, considering $I_0(p_e,n)$ in Equation (9) equal to $I(p_e \pm \delta,n)$, that is, to the average of $I(p_e + \delta,n)$ and $I(p_e - \delta,n)$. In this case Equations (9) to (11) can be modified to

$$\overline{A}(p,\delta,n) = \log[I(p \pm \delta,n)/I(p,n)] \qquad (12)$$

$$N_t \sim [\overline{A}(p,\delta,n)]^2\, \varphi[\overline{A}(p,\delta,n)] = \boldsymbol{A}(p,\delta,n) \qquad (13)$$

$$N_{0e} \cong \alpha_{pe}(\theta/\tau_e)\sum_n \boldsymbol{A}(p_e,\delta,n)\,. \qquad (14)$$

In order to avoid confusion between the terms $\overline{A}(p,n)$, $\boldsymbol{A}(p,n)$ and $\boldsymbol{A}(p,\delta,n)$ we suggest defining them as 'absorbance', 'squared absorbance (SA)' and 'BG corrected SA', respectively. Then, the sums in Equations (11) and (14) multiplied by θ are to be notified as 'SA peak area' or 'BG corrected SA peak area'.

3. Experimental

3.1. Instrumentation

The experimental setup includes a continuum light source, a graphite tube atomizer and an Ocean Optics (Dunedin, FL, USA) HR4000 spectrometer[9] connected to a PC (Fig. 2). The grating, with 1200 grooves mm^{-1} and 5 μm spectral slit, provided a FWHM of about 120 pm within the 190–410 nm wavelength range. The radiation spectrum of the continuum light source was registered using a Toshiba 3680 pixel CCD and the Spectra Suit software providing data acquisition every 4 ms.[9]

A deuterium lamp (D2000, Ocean Optics) and Xe arc (L2479, 300 W, Hamamatsu, Welwyn Garden City, UK) were employed as continuum light sources in various experiments. Radiation was focused in the centre of the graphite tube atomizer and on the entrance slit of the spectrometer using two lenses.

The atomization unit with its power supply was built by Cortec (Moscow, Russia), using the unit of the Cortec AAS instrument Z.ETA as a prototype.[10] It provided programmed heating, fast ramp (10 °C ms^{-1}) and stabilization of the temperature of the tube at the atomization stage. The tubes used in the experiments (manufactured by Schunk, Heuchelheim, Germany) are shown in Fig. 3A and their prototype in Fig. 3B. The internal diameter of the tube (1) was 2.5 mm compared with 4 mm in the prototype; the modified tube provided higher temperature ramp for the tube ends and accommodation of the ring-shaped collector made of carbon fibre (Alfa Aesar, Ward Hill, MA, USA) (2) in a

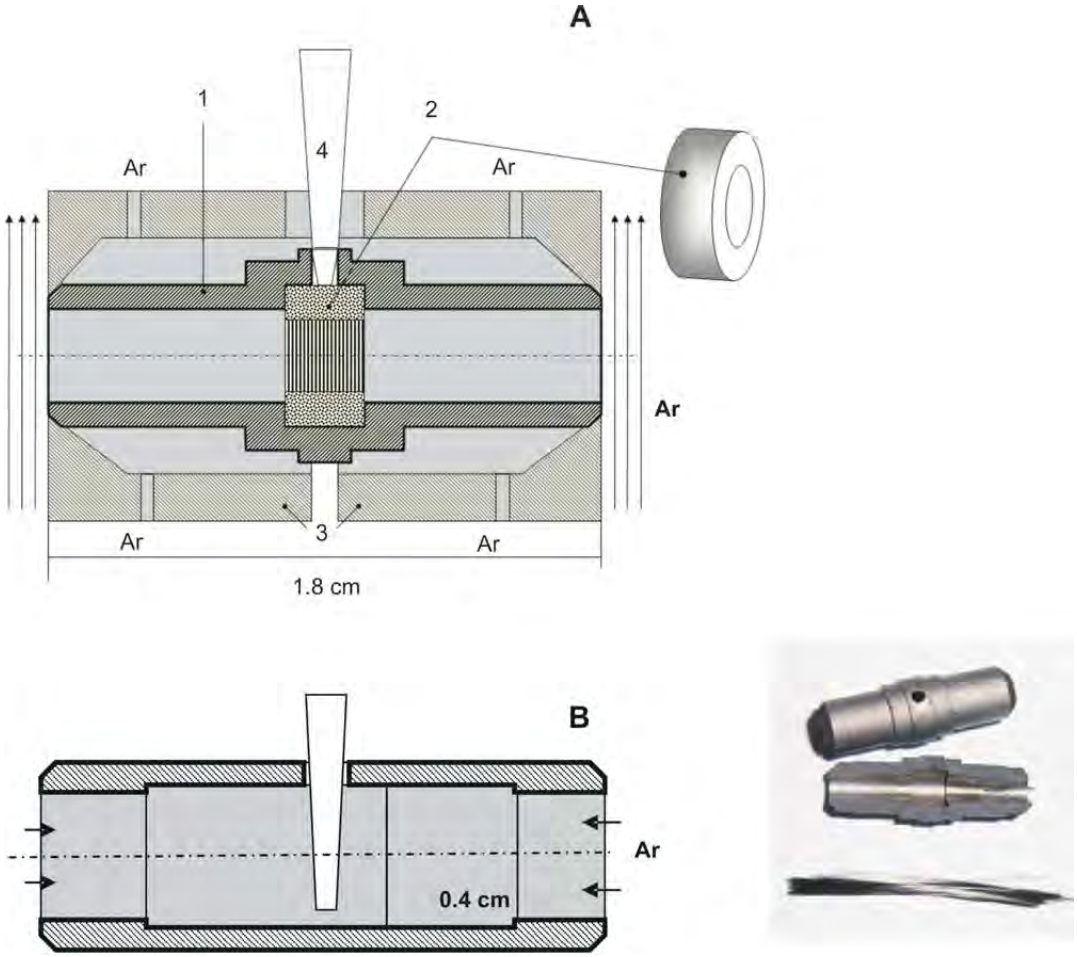

Figure 3 Tube furnace in (**A**) the atomization unit and (**B**) the commercial prototype: pyrocoated graphite tube (1); graphite fibre (collector) (2); electrical contacts (3); and sampling nozzle (4).

special indentation next to the sampling hole.[11] Up to 10 mg of fibre could be accommodated in the tube without shading light. The sampling hole was reduced to 1 mm in diameter; the sample solution was injected directly on the top of the collector using the pipette with sampling tip (4), limiting the depth of entry into the tube. External Ar flow provided protection of the tube from atmospheric gases; supplementary flow near the contacts (3) was directed perpendicular to the tube axis.

3.2. The Samples

The solutions of individual elements and their mixtures were prepared from the reference solutions for AA spectrometry (Industrial Analytical, Kyalami, South Africa) by sequential dilution in 0.2 % nitric acid. The pixel *vs.* wavelength calibration and the selection of the most sensitive analytical lines of Ag, Al, As, Au, Bi, Cd, Co, Cr, Cu, Ga, In, Mg, Mn, Na, Ni, Pb, Sb, Se, Te, Tl and Zn were performed using 10 mg L^{-1} solutions. Of the elements present in the stock solutions as nitrates two mixtures including Ag, Bi, Cd, Ga, In, Mg, Mn, Na, Pb, Tl and Al, Au, Fe, Co, Cr, Cu, Mg, Mn, Ni were composed and diluted to provide a broad concentration range. Both sets of solutions were used separately or as mixtures in the experiments on the evaluation of the determination range.

3.3. Procedure

The measurement procedure included manual sampling, running the temperature programme (Table 1), spectra acquisition during the atomization step and calculations. The settings

Table 1 Temperature programme.

Stage	Temperature/°C	Ramp time/s	Hold time/s	Supplementary Ar flow /mL min^{-1}
Drying	100	10	10	50
Pyrolysis	500–700	1	10	50
Cooling	500	1	1	0
Atomization	2200–2600	0	3	0
Cleaning [a]	2650	1	3	50
Alternative cleaning [b]	3–5 pulses with maximum power heating to 2600 °C and 1s cooling to 300 °C			50

[a] Traditional temperature programme with gas flow through the tube.
[b] Suggested programme with gas flow directed perpendicular to the tube ends.

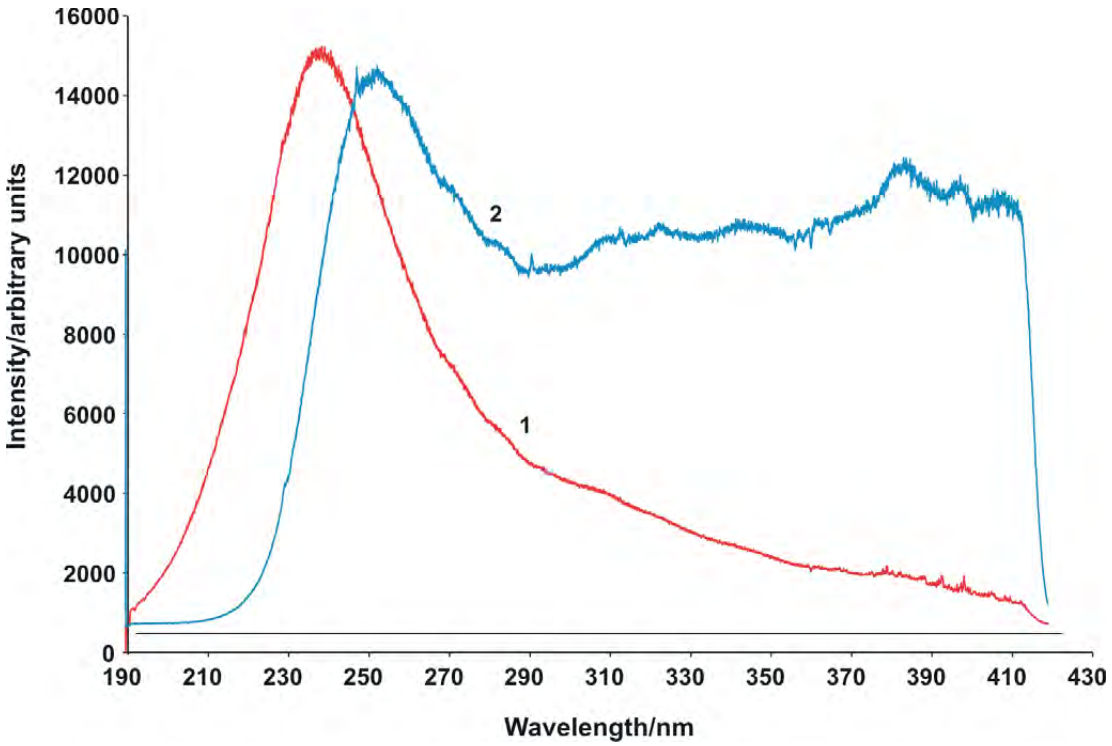

Figure 4 Spectral distribution of the CCD output in the experimental setup with (1) deuterium lamp and (2) Xe arc with fivefold attenuation of radiation; 10 and 4 ms spectra acquisition times, respectively.

2200–2600 °C provided full release of atomic vapour during 1–2 s with gas-stop mode.

The Ocean Optics software employed provided acquisition time of 4 ms or longer and the options regarding averaging the CCD outputs for a certain number of sequential acquisitions. Increase of radiation flux from the light source allowed smaller acquisition time and a higher number of spectra to be acquired during the vaporization pulse. At this stage of research the total number of acquisitions was limited to 80; the averaging option was applied in the case of shorter acquisition times and longer signals. For example, the measurements with D_2 and Xe arc lamps were performed using 8 and 4 ms acquisition times, respectively; with the Xe arc two spectra each were averaged. The data files were opened in Excel worksheets as the tables of CCD outputs. The maximal size of each $I(p,n)$ Excel table was 3680 × 80 cells (190–410 nm wavelength range and 80 spectra obtained). Of those, 18 × 80 cells were used for automatic correction of dark current.

The $I(p,n)$ data were used for the calculation of the squared absorbance (SA), $A(p,n)$, or BG corrected SA, $A(p,\delta,n)$, according to Equations (10) and (13), presentation of signals $A(p_e,n)$ or $A(p_e,\delta,n)$ as functions of time or presentation of peak areas $\theta\sum_n A(p,n)$ or $\theta\sum_n A(p,\delta,n)$ *vs.* wavelength. The spectra obtained for individual elements were employed in the determination of the pixels p_e corresponding to the main absorption lines and the selection of pixels $p_e \pm \delta$ for background correction.

4. Results and Discussion

4.1. Optimization of Experimental Conditions

4.1.1. *Light Source*

The spectral distribution of the electric output of the CCD in the experimental setup for the D_2 and Xe arc lamps is shown in Fig. 4. Graph (1), obtained with 10 ms data acquisition, corresponds to the adjustment of the D_2 lamp to provide the highest output at 190–220 nm. High radiation from the Xe arc lamp permitted the reduction of the data acquisition time to 4 ms ; however, attenuation of the radiation flux was needed because of saturation of the CCD pixels at longer wavelengths. Five times attenuation prevented the saturation above 250 nm but made CCD output at 190–210 nm below measurable level.

4.1.2. *Atomizer*

According to the task, the atomizer should enable the vaporization of various analytes using the single temperature programme, provide complete atomization of molecular species of the analyte, high peak density of atomic vapour and constant residence time of atoms in the gas phase, independent of the volatility of the elements to be determined. The cleaning conditions should guarantee complete removal of sample remnants after the vaporization of large quantities of the analyte. These goals were achieved by modification of the tube furnace, application of a ring-shaped carbon fibre collector instead of the earlier employed solid ballast,[12,13] revision of the temperature programme and redirection of the gas flows.

According to the specification of the Z.ETA spectrometer,[10] the prototype tube furnace provides characteristic masses about five times lower than those obtainable with a transversely heated platform tube atomizer[14] (THGA, Perkin-Elmer, Überlingen, Germany), due to faster heating and the smaller diameter of the absorption volume. Further sensitivity improvement could be expected with the modified tube (see Fig. 3), due to reduction of the internal diameter of the tube and diminishing of vapour losses through the smaller sampling hole partially screened by the collector.

The shape of the tube with a bulge in the centre provides inverted temperature distribution, compared with the prototype, and faster heating of the tube ends (Fig. 5A). Apparently, vapour transportation out of the tube through the high temperature areas provides more efficient atomization.

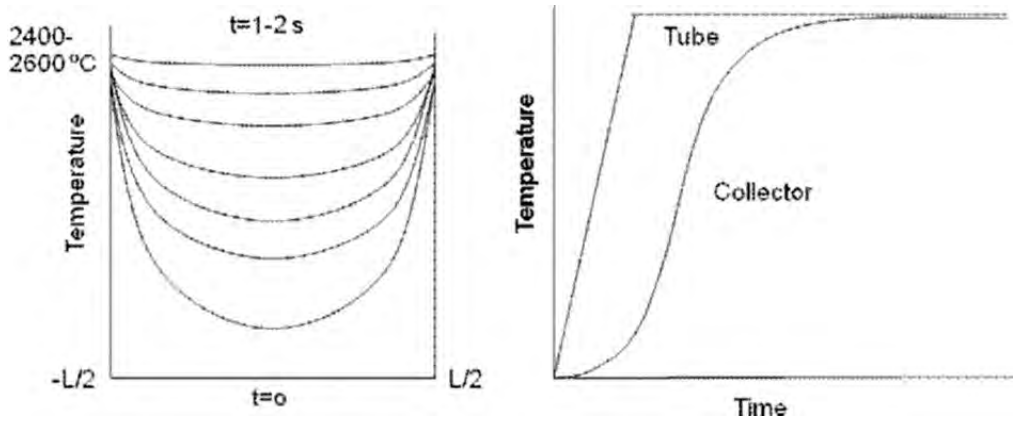

Figure 5 Anticipated temporal distribution of temperature (**A**) along the tube, and (**B**) in its centre between the wall and the collector.

The ring of graphite fibre located next to the tube wall in the special indentation (Fig. 3) serves as a collector, making possible accommodation of 10 μL of the sample solution in the centre of the tube. The collector combines large surface, over which dry residue of the sample is distributed after the drying stage, low heat conductivity in the radial direction and relatively small area of the surface exposed to radiation from the tube wall. These factors effectively delay the vaporization (Fig. 5B), which helps to increase the degree of atomization. Although the collector works similarly to the platform in the THGA[8] or ballast in the smaller tube,[12,13] its design makes possible substantial reduction of the mass of the tube and the diameter of the absorption volume. These factors in turn affect the heating rate and vapour density. Fast heating of the tube ends facilitates the positive effect of the collector.

The vaporization lag depends on the amount of carbon fibre introduced in the tube, the level of temperature stabilization and the volatility of the analyte. A temperature of 2600 °C and a 2.5 mg collector provide the conditions necessary for the determination of all analytes listed above, from Cd to Co and Ni. The atomization pulses for individual elements injected as 13.3 mg L^{-1} solutions in the tube furnished with 2.5 mg of fibre and heated to 2200 and 2600 °C are shown in Figs. 6 and 7 respectively (the elements are listed in the figures according to the appearance of peak maxima); the signals are normalized to equal height; the dots outlining the vaporization pulses indicate the moments of data acquisition.

It can be seen from Fig. 6 that the 2.5 mg collector and relatively low level of temperature stabilization provide the lag sufficient for vaporization and vapour transport of volatile elements at a nominal constant temperature of 2200 °C. The signals for Na, Mg and Mn in Fig. 6 show that higher temperature is needed for faster vapour release to improve signal to noise ratio. The same collector will hardly provide sufficient lag for highly volatile elements if the atomization temperature is set equal to 2600 °C. If simultaneous determination of highly and less volatile elements is needed, a temperature of 2600 °C should be applied, the mass of the collector increased or chemical modification additionally employed. Since further optimization of the collector needs special attention, the investigation in this work was restricted by general problems and the characteristics of the method.

4.1.3. *Atomization Unit and Temperature Programme*

When a constant temperature of 2650 °C and gas flows through the tube were applied for the cleaning in compliance with traditional ET AAS methodology, 'memory' signals were observed

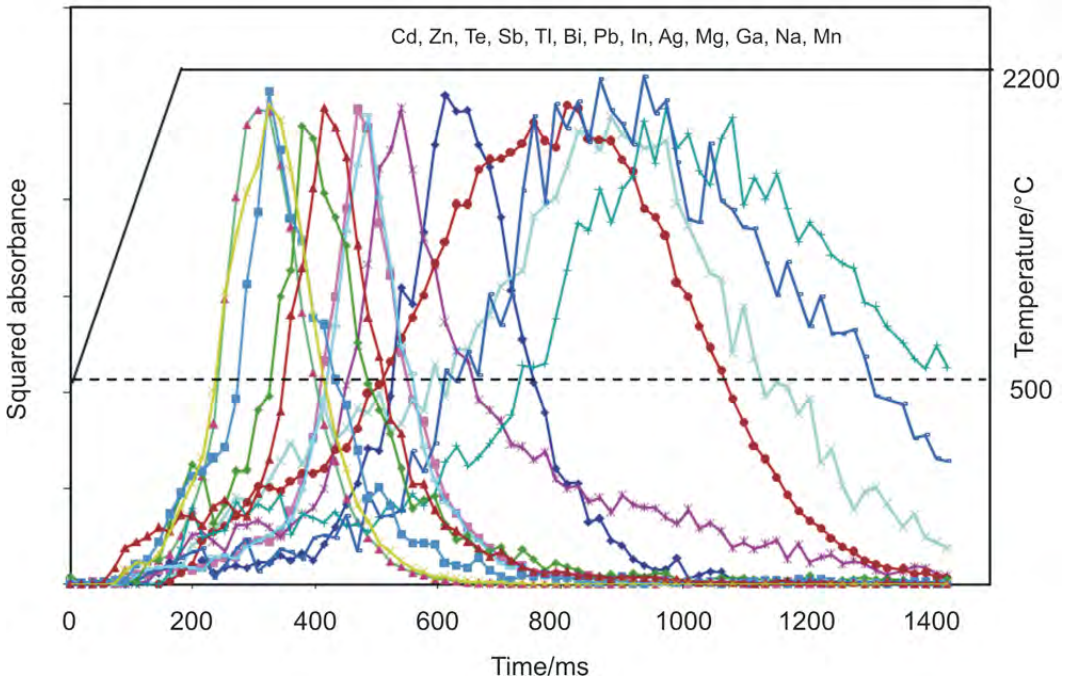

Figure 6 Atomic absorption of elements of high and medium volatility normalized by peak height; atomization temperature 2200 °C.

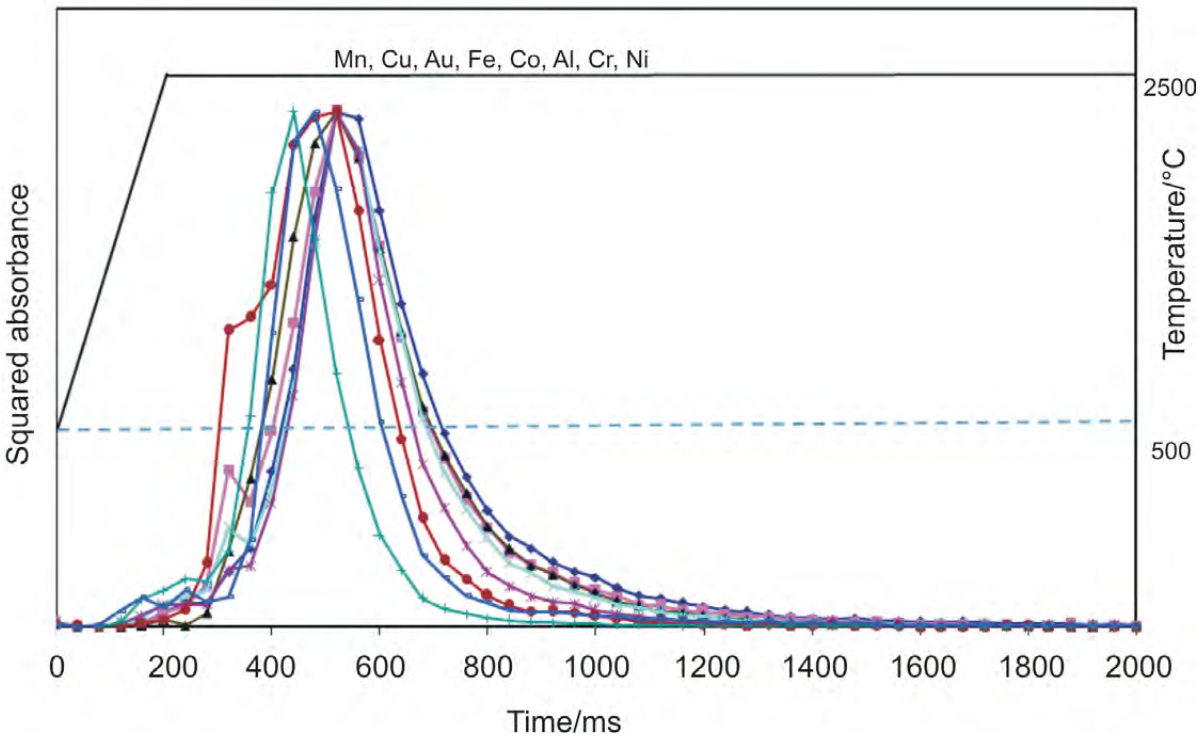

Figure 7 Atomic absorption of medium volatility elements normalized by peak height; atomization temperature 2600 °C.

after the vaporization of large amounts of the analyte. A typical 'memory' signal for Mg is shown in Fig. 8, curve 1. The first dominating mode of the signal appeared prior to that associated with the vaporization from the collector (Fig. 6, Mg signal) that made evident partial condensation of the analyte at the ends of the tube. High cleaning temperature combined with gas flow through the tube did not provide satisfactory removal of the 'memory' signals.

The 'memory' effect was eventually reduced by introducing the changes in the temperature programme (Table 1) and the direction of the cleaning gas flow. The cleaning was performed by a sequence of heating pulses with fast maximum power ramp, similar to that applied at the atomization stage, and interim cooling periods (see Fig. 9). This mode of operation made possible predominant heating of the tube ends during the cleaning stage.

The design of the atomization unit was changed to direct the gas flows during the drying, pyrolysis and cleaning stages through the narrow channels near the tube ends perpendicular

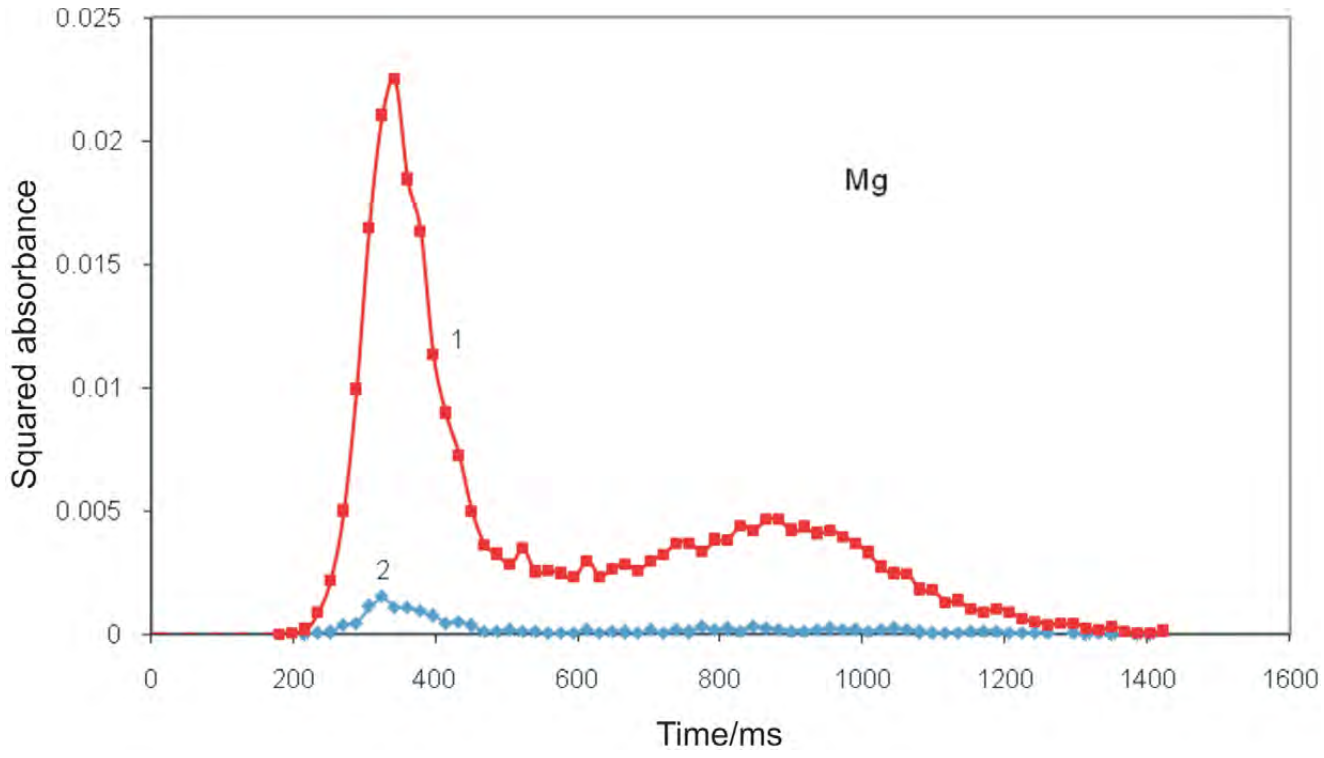

Figure 8 Memory signal observed during blank run of temperature programme after the vaporization of 0.1 μg Mg with (1) traditional and (2) suggested cleaning procedures, including five heating pulses.

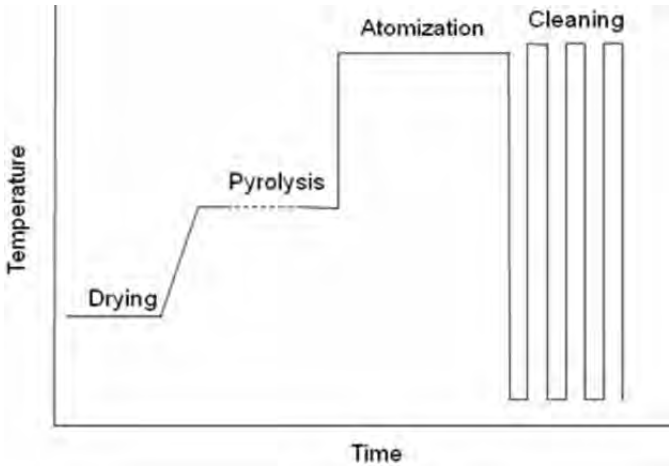

Figure 9 Diagram of the temperature programme.

to the tube axis. The sample constituents or re-evaporation products released from the collector and tube ends were sucked out of the tube on account of the Venturi effect.[15] With the listed improvements introduced the 'memory' signals of Mg became negligible after 3–5 cleaning pulses at a temperature of 2600 °C (Fig. 8, curve 2).

4.2. Analytical Performance

4.2.1. *Absorption Spectra of Individual Elements, Spectral Interferences and BG Correction*

The absorption spectra of individual elements observed consisted mainly of atomic lines, however, in some cases molecular bands belonging to dimers, gaseous oxides or carbon-containing molecules could be observed for the samples with high analyte content. An example of a combination of atomic lines and molecular bands in the vapour spectrum of Al is presented in Fig. 10A. The persistence of the molecular band at 250–270 nm, attributed to Al_2O,[16] shows that full atomization is not yet achieved for the samples having stable molecules in the gas phase. The spectrum reported in Fig. 10A was calculated according to Equation (9) using blank and sample measurements. By contrast, only atomic lines are seen in the spectrum (Fig. 10B) calculated from the data of a single sample measurement according to Equation (12), where $\delta = 3$. Apparently, the correction method applied is viable for the background continuum or molecular bands broader than atomic lines.

The manganese absorption spectrum (lines at 279.482, 279.827 and 280.108 nm) in Fig. 11A illustrates the properties of the experimental setup, regarding spectral resolution, in comparison with a HR CS instrument (Fig. 11B, from Ref. 2). The estimated FWHM for the first line of the triplet is 60 times higher than that for the HR CS spectrometer.

Direct comparison of sensitivities for HR and LR AA spectrometers is not possible because of differences in the calculation algorithms, but at least 60 times reduction of sensitivity with similar atomizers is to be expected for LR, according to the FWHM ratio. This deficiency was expected to be partially counterbalanced by sensitivity improvement with the use of the atomizer (see Fig. 3).

The most sensitive lines of volatile and less volatile elements observed in this work are listed in Table 2 as two groups; the wavelengths in the Table are indicated according to the HR data.[2] For all elements except Zn, Cd and Se the spectra observed contain two or more outstanding lines. The peak areas

Table 2 The determination sensitivity of volatile and less volatile elements, and its anticipated change due to the superposition of absorption spectra of other elements in the respective group.

Element [a]	λ/nm	$\theta\sum A(p_e,\delta=3,n)$/ ms per 0.1 g of the analyte		I/II
		I. Spectrum of individual element	II. Superimposed spectra	
Ag	328.068	3.35	3.56	0.94
Ag	338.289	1.21	1.34	0.90
As	193.696	0.56	0.40	1.39
As	197.197	3.00	0.54	5.55
Bi	223.061	3.02	2.55	1.19
Bi	306.772	1.12	1.21	0.92
Cd	228.802	18.72	18.80	1.00
Ga	287.424	4.21	3.64	1.16
Ga	294.364	6.73	6.67	1.01
In	303.936	5.30	5.15	1.03
In	325.609	1.78	1.90	0.94
Mg	285.213	61.10	59.23	1.03
Na	330.237	3.66	3.63	1.01
Pb	217.001	5.59	5.23	1.07
Pb	283.306	2.29	2.42	0.95
Sb	217.581	1.96	1.25	1.57
Sb	231.147	2.57	1.05	2.45
Se	196.026	0.20	0.17	1.13
Te	214.281	1.87	1.65	1.14
Tl	237.958	2.56	2.06	1.24
Tl	276.787	5.15	5.00	1.03
Zn	213.857	18.97	18.38	1.03
Al	237.312	3.52	3.55	0.99
Al	226.91	4.13	4.07	1.01
Al	309.27	2.60	2.63	0.99
Au	242.795	3.52	3.55	0.99
Au	267.595	0.45	0.91	0.50
Co	240.725	2.15	2.16	1.00
Co	241.162	1.34	1.32	1.01
Co	242.493	1.15	1.10	1.05
Cr	236.591	0.38	0.41	0.92
Cr	298.647	0.16	0.16	0.99
Cr	301.492	0.25	0.20	1.21
Cu	324.754	0.98	0.96	1.02
Cu	327.396	0.43	0.42	1.03
Fe	248.321	25.34	25.77	0.98
Fe	249.064	9.92	9.88	1.00
Fe	252.285	7.97	7.97	1.00
Fe	302.064	11.05	11.25	0.98
Mn	279.482	5.97	5.93	1.01
Mn	279.827	4.25	4.70	0.90
Mn	280.108	3.02	3.20	0.95
Ni	231.096	0.70	0.69	1.02
Ni	232.003	1.50	1.76	0.85

[a] Measured using 10 mg L^{-1} solutions of individual elements.

$\theta\sum_n A(p,\delta,n)$, where $\delta = 3$ measured for equal concentrations (10 mg L^{-1}) of the analytes, are reported in the third column of Table 2, which permits evaluation of the relative sensitivities for various lines.

The reduced resolution increases the probability of spectral interferences due to possible overlap of the absorption lines indicated in Table 2 with the lines of the elements present in the sample. For elements of different volatility reduction of mutual

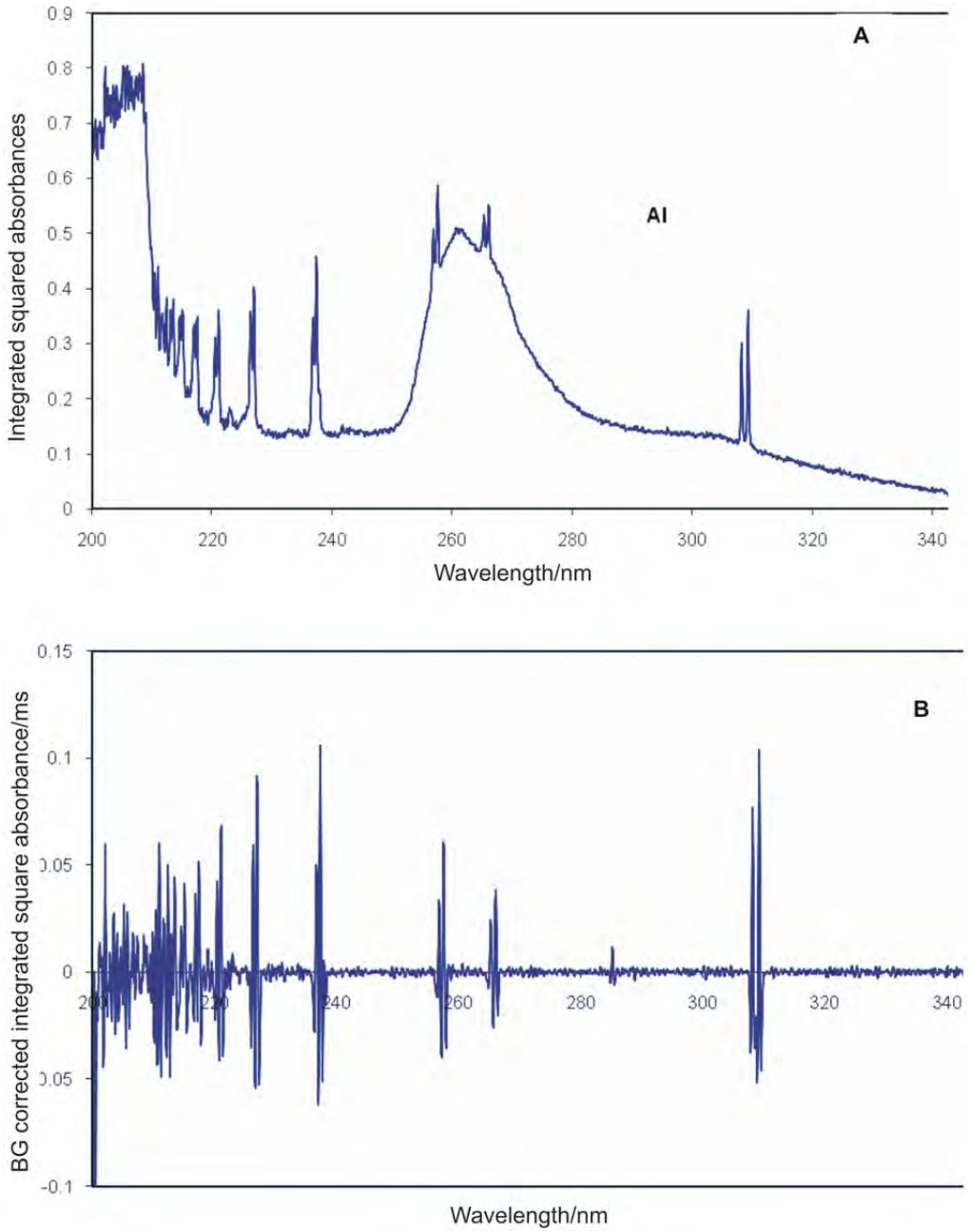

Figure 10 Vapour absorption spectrum for the sample 0.1 μg Al calculated according to (**A**) Equations (9) to (11), and (**B**) Equations (12) to (14), where δ =3.

interferences by optimization of the detection time and modification of the temperature programme can be expected. The probability of spectral interferences for equal amounts of analytes of similar volatility can be evaluated by comparison of the signals at the pixels corresponding to the lines in Table 2 in the presence and absence of other elements. According to this suggestion the absorption spectra of various elements observed with a deuterium lamp (14 and 8 spectra of the elements of the first and second groups in Table 2, respectively) were summarized and the sums (fourth column of Table 2) compared with the absorption of individual elements. The results are reported in the fifth column of Table 2. It is seen that for most of the analytical lines the ratios of peak areas with/without potential interfering lines are close to unity. For the wavelengths below 210 nm the suggested criterion of evaluation is hardly applicable because of high short noise due to low radiation. The fluctuations can also cause small deviations of the measured ratio from unity. Thus, the data presented show that the problem regarding the overlapping of atomic absorption lines, in general, should not affect multi-element determination. Obviously, there are some exceptions for specific elements (e.g. for Tl, Sb, Au and Ni); in some of these cases the alternative lines can be employed.

4.2.2. *The Determination Range and Limits of Detection*

The determination ranges for various elements were defined in two sets of experiments. In the first set the samples employed were prepared by sequential dilution of two stock solutions, Ag, Bi, Cd, Ga, In, Mn, Pb, Tl and Al, Fe, Co, Cr, Cu, Ni, Mg, Mn. The calibration curves $\theta\sum_n A(p,\delta=3,n)$ *vs.* log (N_{0e}) obtained with these solutions are shown in Fig. 12. The graphs can be approximated by straight lines $Y = aX + C$ extended within 3.5 to 4.5 orders of magnitude with coefficients a specific for each element

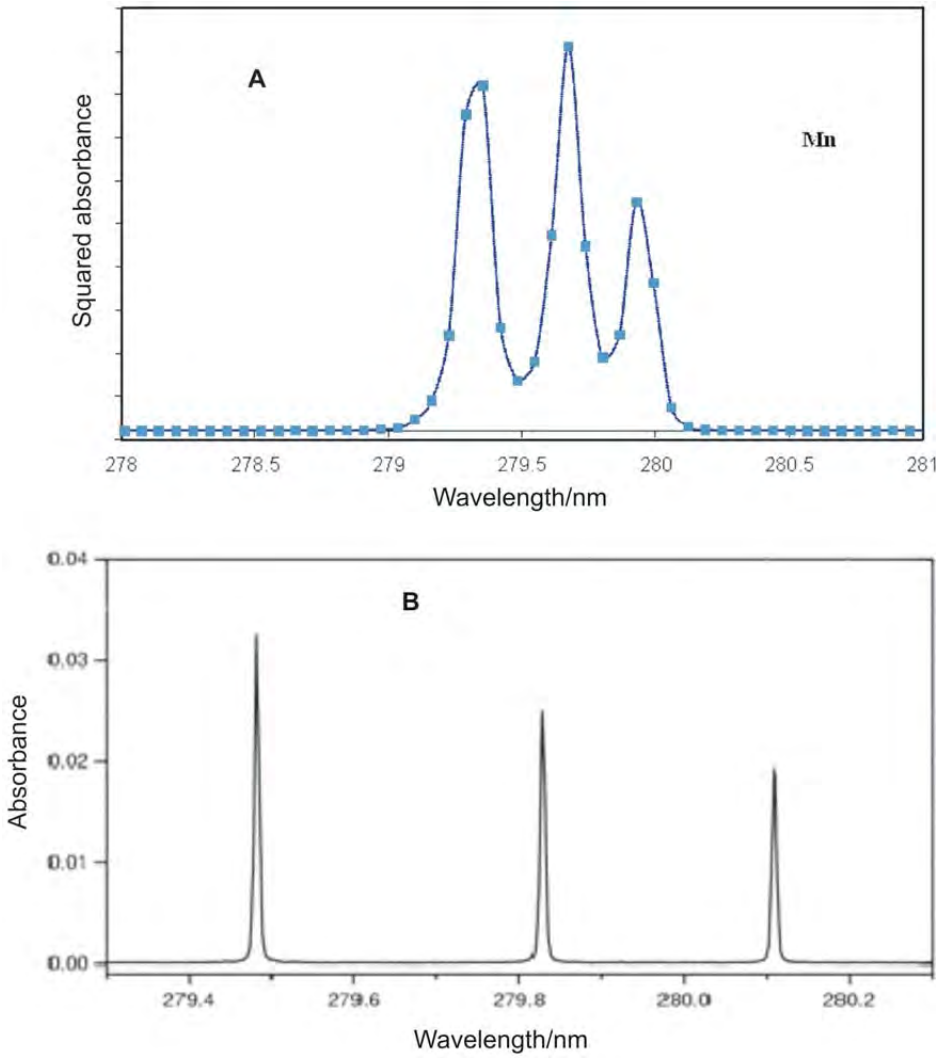

Figure 11 Mn triplet at 279.482, 279.827 and 280.108 nm observed in (**A**) the experimental setup, and (**B**) the HR AA spectrometer.[2]

between 0.67 and 0.95. The deviation from the theoretical value, unity, is most probably related to incomplete atomization for the larger amounts of the analyte or vapour losses due to migration of metals into pyrocoated graphite.[18]

In a second set of experiments the diluted mixtures of volatile elements were sampled together with the solution of the mixture of elements having complicated atomic spectra (Al, Fe, Co, Cr, Cu, Mg, Mn and Ni, 33 mg L^{-1} of each metal). In this case the linearity ranges of the respective calibration curves depended on the absorption lines employed. Typical calibration curves for Tl lines are shown in Fig. 13: line Tl 276.8 nm can be used within 3.5 orders of magnitude determination range and up to 33 000-fold excess of matrix; the parameters for the Tl 237.9 nm line are limited by 2 orders of magnitude range and 1000 times matrix excess. For other volatile elements the best analyte to matrix mass ratio deviated between 6000 and 33 000, as for Pb in Fig. 14.

In the presence of the matrix the absorbance signals for volatile elements were shifted towards longer time, as shown in Fig. 15 for Cd and Ga. The slopes of the calibration curves for all volatile metals were close to unity, which indicated increases of the degree of atomization.

The limit of detection (LOD) for different elements was considered as the concentration that caused the BG corrected SA peak area equal to 3 standard deviations (SD) of blank measurements. The SD values were calculated from the data acquired in 10 blank measurements and the respective LODs were evaluated according to the calibration curves (see Fig. 12). The LOD for 10 μL injected volumes are compared in Table 3 with the data for the traditional flame AAS and OE ICP with radial and axial

Table 3 Limits of detection for SMET AAS and ICP OES methods.

Element	LOD/μg L^{-1}			
	SMET AAS [a]	Flame AAS (Varian) [b]	ICP (Varian) [b]	ICP (Spectro)[c]
Ag	0.7	2	3.0	1.20
Al	2.7	30	1.5	0.11
Au	8.2	10	5.5	–
Bi	1.1	50	12.0	–
Co	12.0	5	5.0	0.94
Cr	0.4	6	4.0	0.02
Cu	4.0	6	2.0	1.40
Fe	2.1	6	1.5	0.50
Ga	3.2	100	0.5	–
In	0.9	40	18.0	–
Mn	3.0	2	0.3	0.11
Ni	4.3	10	5.5	1.10
Pb	0.9	10	14.0	6.90
Tl	0.1	20	16.0	6.50

[a] 10 μL injected.
[b] Ref. 19.
[c] Ref. 20.

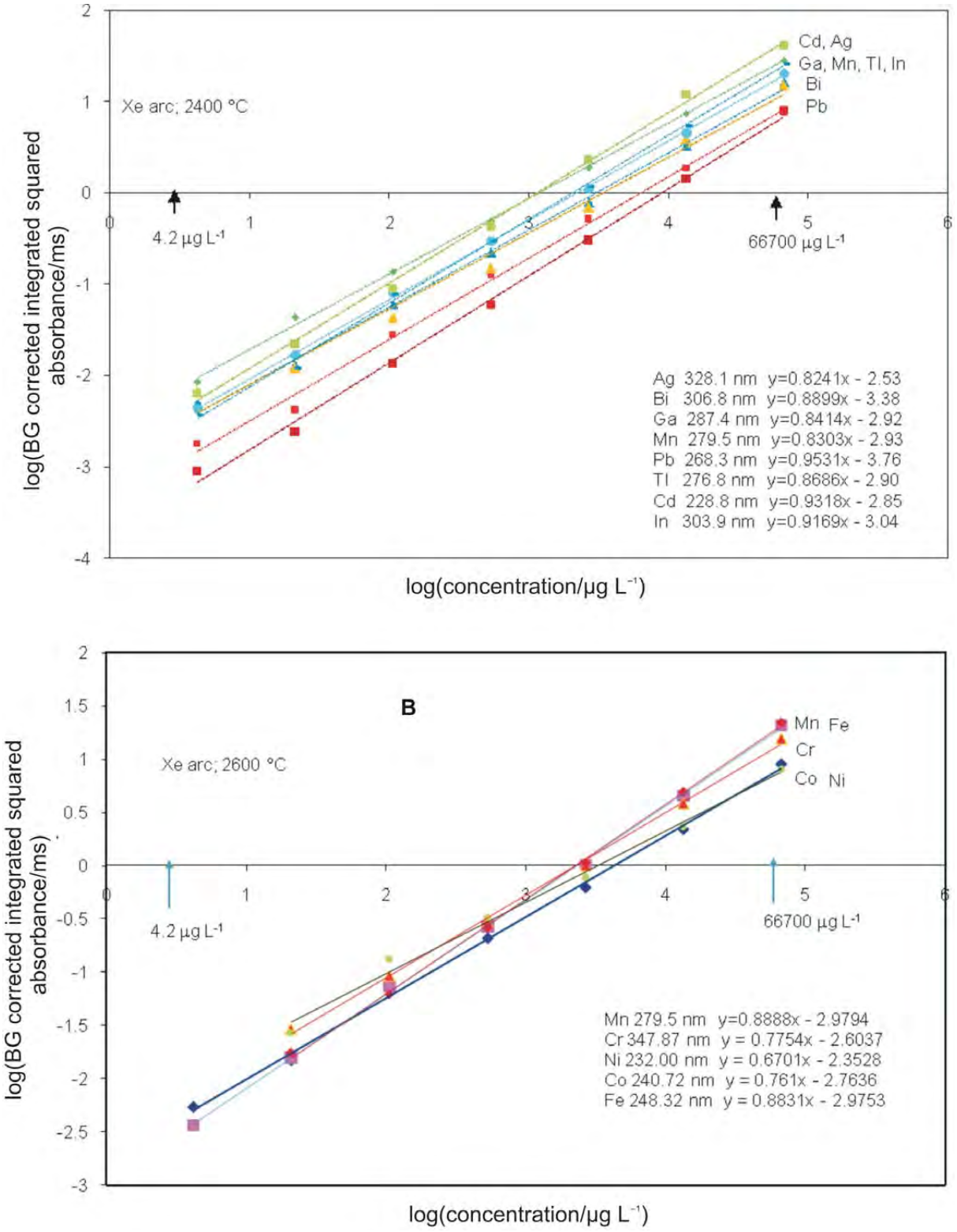

Figure 12 Simultaneous determination of (**A**) volatile and (**B**) less volatile elements in the solutions containing equal concentrations of the analytes in water: calibration curves for individual elements.

plasma observation.[19,20] It is seen that for almost all elements the LODs found in this work are lower than those for flame AAS and comparable with those for ICP. It should be also kept in mind that LODs in SMET AAS can be substantially reduced, compared with those in Table 3, on account of the optimization of the detection time for each element, multiple sample injection or selection of temperature programme for the group of elements of similar volatility.

5. Conclusions

The validity of the suggested method of simultaneous multi-element ET AAS determination has been justified. The method is less sensitive than traditional ET AAS but rapidity of analysis, broad range of concentrations available for determination, LODs close to those in flame AA with clear prospects of improvement, simplicity and, therefore, low cost of the instrumentation distinguish SMET AAS from other instrumental

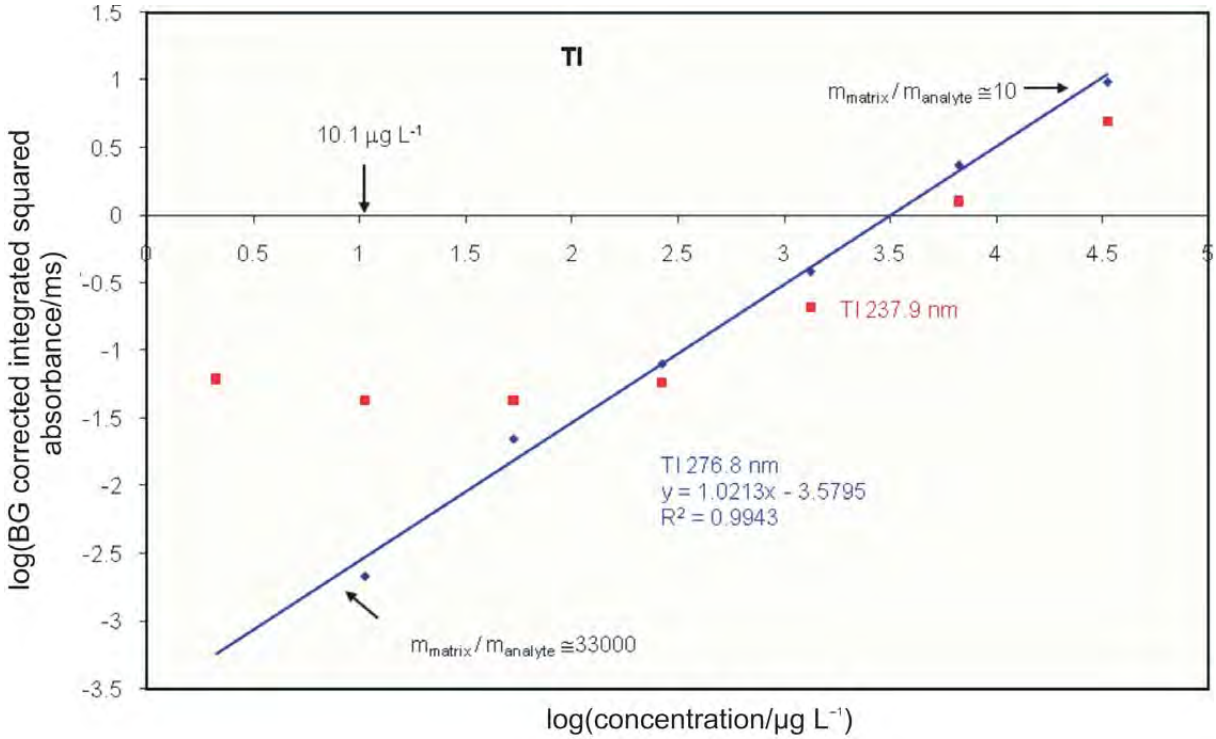

Figure 13 Simultaneous determination of Ag, Cd, Bi, In, Ga, Pb and Tl in the solutions containing in total 264 mg L^{-1} of Al, Co, Cr, Cu, Fe, Ni, Mg and Mn (33 mg L^{-1} of each metal): calibration curves for Tl.

methods. The problems regarding optimal detection of the absorption signals of different elements, spectral and chemical interferences still need thorough investigation. The results at this stage of research permit the suggestion that SMET AAS can find broad application in those fields where flame AAS is still extensively used. Apart from the analytical advantages regarding fast analysis of unique samples, determination of element ratios, internal standardization of injected masses, and others, e.g. the substitution of flame by electrothermal atomization, should permit the elimination of specific safety problems connected with storage and the use of flammable gases. The anticipated further reduction of LODs on account of brighter light sources, faster electronics and further improvement of the atomization technique should broaden the field of SMET AAS applications.

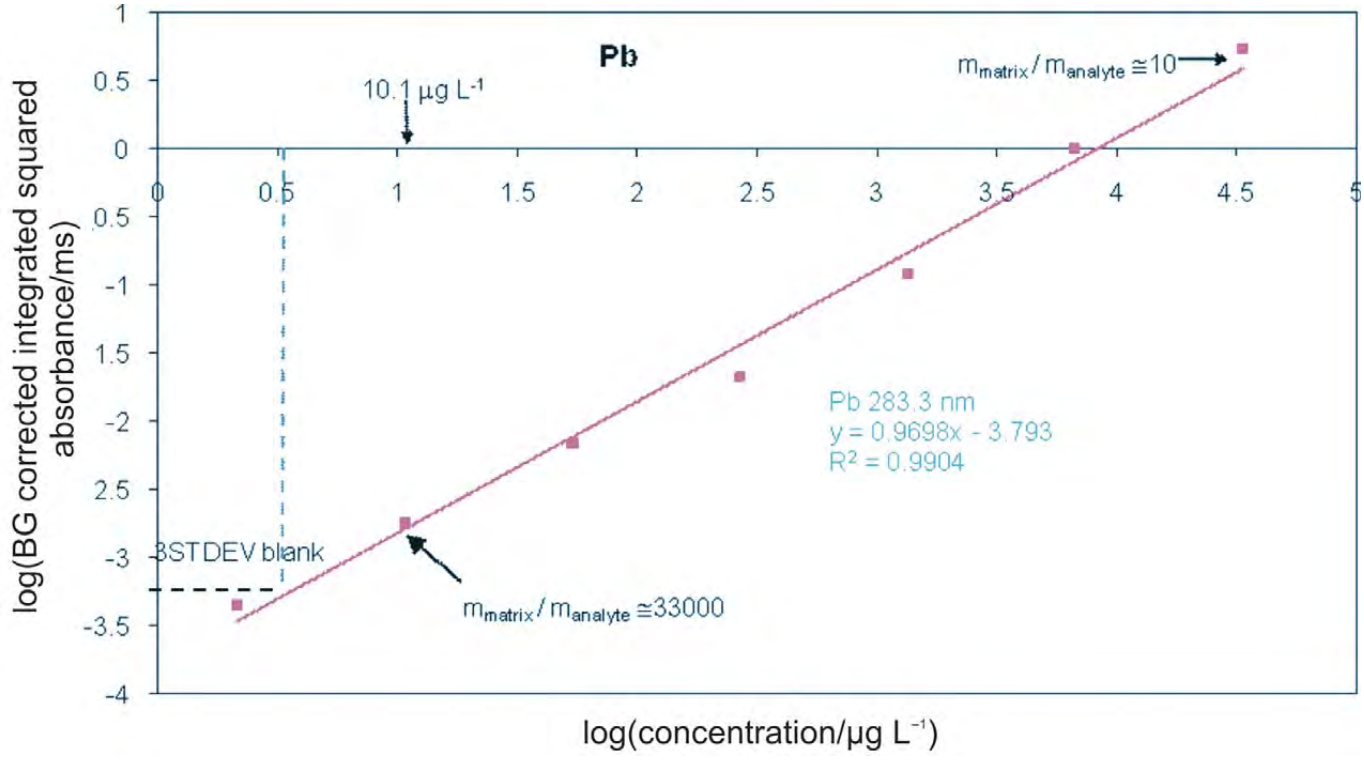

Figure 14 Simultaneous determination of Ag, Cd, Bi, In, Ga, Pb and Tl in the solutions containing in total 264 mg L^{-1} of Al, Co, Cr, Cu, Fe, Ni, Mg and Mn (33 mg L^{-1} of each metal): calibration curves for Pb.

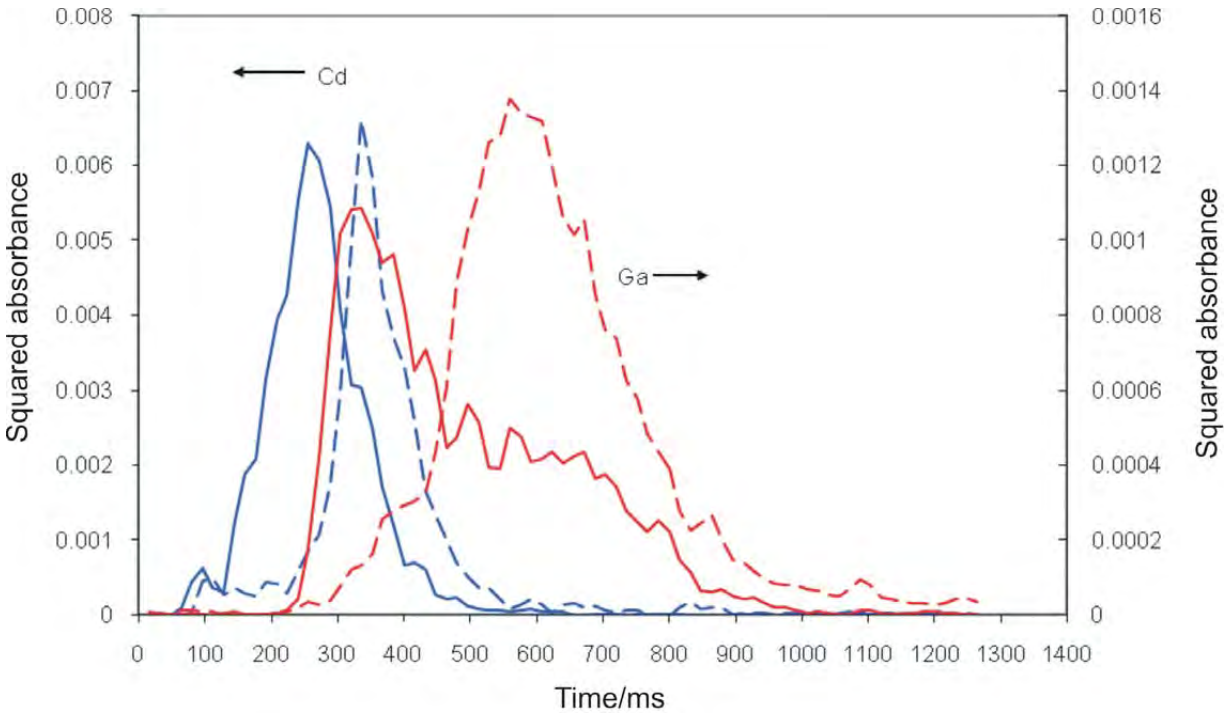

Figure 15 Simultaneous determination of Cd and Ga in the solutions containing 0.66 mg L^{-1} of Ag, Cd, Bi, In, Ga, Mg, Mn, Pb and Tl (solid lines) and, additionally, 33 mg L^{-1} each of Al, Fe, Co, Cr, Cu, Mg, Mn and Ni (dashed lines).

Acknowledgements

The authors would like to acknowledge the National Research Foundation, South Africa, and Tshwane University of Technology for financial support of this research.

References

1 J.M. Harnly, *J. Anal. At. Spectrom.*, 1999, **14**, 137–146.
2 B. Welz, H. Becker-Ross, S. Florek and U. Heitmann, *High-resolution Continuum Source AAS: The Better Way to do Atomic Absorption Spectrometry,* Wiley-VCH, Weinheim, Germany, 2005.
3 http://www.analytik-jena.de (accessed 1 March 2010).
4 U. Heitmann, H. Becker-Ross and D. Katskov, *Spectrochim. Acta, Part B,* 2006, **61**, 351–360.
5 B.V. Lvov, *Atomic Absorption Spectrochemical Analysis,* Adam Hilger, Elsevier, London, UK, 1970.
6 K.I. Tarasov, *The Spectroscope,* Adam Hilger, Bristol, UK, 1974.
7 A.C.G. Mitchell and M.W. Zymansky, *Resonance Radiation and Excited Atoms,* Cambridge University Press, Cambridge, UK, 1961.
8 B. Welz and M. Sperling, *Atomic Absorption Spectrometry,* 3rd edn., Wiley-VCH, Weinheim, Germany, 1999.
9 http://www.OceanOptics.com (accessed 1 March 2010).
10 http://www.cortec.ru (accessed 1 March 2010).
11 RSA Provisional Patent Application 2008/06901.
12 D.A. Katskov, *J. Anal. At. Spectrom.*, 2005, **20**, 220–226.
13 D.A. Katskov, Yu. M. Sadagov and M. Banda, *J. Anal. At. Spectrom.*, 2005, **20**, 227–232.
14 *SIMAA 6000 Simultaneous Multi-element Atomic Absorption Spectrometer,* Perkin-Elmer Bodenseewerk, Überlingen, Germany, 1995.
15 http://en.wikipedia.org (accessed 1 March 2010).
16 D.A. Katskov, A.M. Shtepan, I.L. Grinshtein and A.A. Pupyshev, *Spectrochim. Acta, Part B,* 1992, **47**, 1023–1041.
17 http://physics.nist.gov (accessed 1 March 2010).
18 J.G. Jackson, R.W. Fonseca and J.A. Holcombe, *Spectrochim. Acta, Part B,* 1995, **50**, 1837–1846.
19 G. Tyler, *VARIAN Instruments at Work. Application Note. AA or ICU: Which Do You Choose?* ICP-3, Varian Inc., Mulgrave, Victoria, Australia, 3 September 1991.
20 P. Heitland, Spectro ICP Report No. ICP-32, Spectro Analytical Instruments, Kleve, Germany, 2001.